Available online at www.sciencedirect.com

ScienceDirect

Chinese Journal of Natural Medicines 2019, **17**(11): 0842–0857

Chinese Journal of Natural Medicines

•Special topic•

Profiling the metabolites of astrapterocarpan in rat hepatic 9000*g* supernatant

ZHANG Ya-Zhou [1, 2], XU Feng [1*], DONG Jing [3], LIANG Jing [1], HASHI Yuki [3], LIU Guang-Xue[1], LI Yao-Li [1], SHANG Ming-Ying [1], WANG Xuan [1], CAI Shao-Qing [1*]

[1] *State Key Laboratory of Natural and Biomimetic Drugs, School of Pharmaceutical Sciences, Peking University, Beijing 10000, China;*

[2] *School of Pharmaceutical Sciences, Guizhou University, Guiyang 550000, China;*

[3] *Shimadzu China MS Center, Beijing 10000, China*

Available online 20 Nov., 2019

[ABSTRACT] Astrapterocarpan (AP) is a bioactive constituent of Astragali Radix and was selected as a model compound for investigating the *in vitro* metabolism of pterocarpans in this study. Its *in vitro* metabolism was conducted by incubation with rat hepatic 9000*g* supernatant (S9) in the presence of an NADPH-generating system. At first, four compounds were isolated and their structures were elucidated as 6a-hydroxy-AP (**M1**), astrametabolin I [**M2**, 1a-hydroxy-9, 10-dimethoxy-pterocarp-1(2), 4-diene-3-one], 9-demethyl-AP (**M3**, nissolin) and 4-methoxy-astraisoflavan (**M4,** 7, 2′-dihydroxy-4, 3′, 4′-trimethoxy-isoflavan) on the basis of NMR data, respectively. Among them, **M1**, **M2** and **M4** were new compounds. Next, the metabolite profile of AP in rat hepatic S9 was obtained *via* HPLC-DAD-ESI-IT-TOF-MS^n, and 40 new metabolites were tentatively identified. These newly identified metabolites included 9 monohydroxylated metabolites, 1 demethylated metabolite, 7 demethylated and monohydroxylated metabolites, 4 dihydroxylated metabolites, 1 hydration metabolite, 1 didemethylated metabolite, 2 glucosylated metabolites, 1 monohydroxylated and dehydrogenated metabolite, 2 monohydroxylated and demethylated and dehydrogenated metabolites, 2 dimerized metabolites, 3 dimerized and monohydroxylated metabolites, 2 dimerized and didemethylated metabolites, and 5 dimerized and demethylated metabolites. Finally, the major metabolic reactions of AP in rat hepatic S9 were summarized and found to be hydroxylation, demethylation, dimerization, hydration, and dehydrogenation. More importantly, the biotransformation from AP to **M2** and the dimerization of AP by incubation with hepatic S9 were reported for the first time. In conclusion, this is the first report on the metabolism of a pure pterocarpan in animal tissues, and these findings will provide a solid basis for further studies on the metabolism of other pterocarpans.

[KEY WORDS] Pterocarpan; Astragali Radix; LCMS; Hepatic S9; Metabolism

[CLC Number] R917 **[Document code]** A **[Article ID]** 2095-6975(2019)11-0842-16

Introduction

Astrapterocarpan (AP, Fig. 1) is a bioactive constituent of Astragali Radix (a commonly used traditional Chinese drug [1][2]), which has also been isolated from other medicinal plants, such as *Lathyrus nissolia* [3], *Dalbergia odorifera* [4], *Medicago sativa* [5], *Sphaerophysa salsula* [6], *Oxytropis kansuensis* [7], and *Clinopodium urticifolium* [8].

It is a phytoalexin [3], and can inhibit sterol biosynthesis [9], promote bone formation [10], inhibit proliferation of vascular smooth muscle cells and atherogenesis [11]. Recently, the inhibition effect of its 3-*O*-glucoside on concanavalin A-induced T lymphocyte proliferation has been reported [12].

In previous studies, we have discovered that: (1) AP-3-*O*-glucuronide and AP-3-*O*-sulfate can be detected in the pig serum after orally administrated with Buyang Huanwu decoction whose major component is *Astragali* Radix [13]; (2) AP in Astragali Radix decocotion can be absorbed in rat everted gut sac model; (3) pterocarpans in Astragali Radix decocotion can be metabolized to AP-3-*O*- -D-glucuronide by small intestine during absorption; (4) AP-3-*O*- -D-glucuronide can be de-

[Received on] 1-Oct.-2019

[Research funding] This work was supported by the National Natural Science Foundation of China (No. 81673595) and China Postdoctoral Science Foundation (Nos. 20080430293 and 200902040), and Guizhou Natural Science Foundation (No. QIANKEHE [2018]1071).

[*Corresponding author] E-mail: xufeng76@hsc.pku.edu.cn (XU Feng); sqcai@ hsc.pku.edu. cn (CAI Shao-Qing)

These authors have no conflict of interest to declare.

tected in the urine of human orally administrated with Astragali Radix decocotion [14]. It is reported that a hydroxylated AP can be detected in the urine [15] and a dehydrogenated metabolite [16] can be detected in the bile of the rats dosed with Danggui Buxue Tang which consists of Astragali Radix and Angelicae Sinensis Radix. Hence, only four potential metabolites (produced in animals) of AP have been known so far; they are AP-3-*O*-glucuronide, AP-3-*O*-sulfate, hydroxylated AP-3-*O*-glucuronide and dehydrogenated AP-3-*O*-glucuronide.

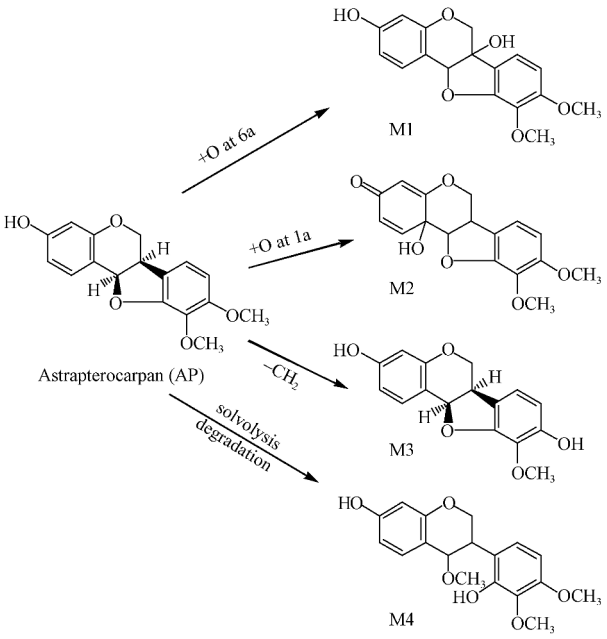

Fig. 1 Structures of astrapterocarpan and its four products formed in rat hepatic S9

However, we found that the generation of these four metabolites from AP lacks direct evidence, because the dosed drugs are not pure astrapterocarpan in all these reports. Furthermore, there are no reports on the *in vitro* metabolism of AP or pterocarpans by animal tissues in literature. Therefore, we chose AP as a model compound to investigate the *in vitro* metabolism of pterocarpans by animal tissues. Specifically, the *in vitro* phase I metabolism of AP by rat hepatic S9 was studied for the first time, and the metabolic pathways of AP were proposed based on the metabolites identified by spectroscopic analysis and HPLC-DAD-ESI-IT-TOF-MS^n analysis.

Materials and Methods

Chemicals and reagents

AP (Molecular formula: $C_{17}H_{16}O_5$, exact molecular weight: 300.0998 Da) was isolated by the authors from Astragali Radix [the roots of *Astragalus membranaceus*] *via* chromatographic methods [17], including column chromatography on D-101 macroporous adsorption resin (Cangzhou Baoen Co., Ltd., Hebei Province, China), 200–300 mesh normal phase silica gel (Qingdao Marine Chemical Factory, Qingdao, Shandong Province, China), reversed phase C_{18} silica gel (YMC, YMC Co., Ltd., Japan) and Sephadex LH-20 (GE Healthcare Co., Ltd., USA). And its structure was determined to be (6a*R*, 11a*R*)-3-hydroxy-9, 10-dimethoxy-pterocarpan [11] on the basis of UV, NMR, and MS data. Its purity was determined to be > 98% by area normalization method at 280 nm using HPLC-DAD analysis. HPLC-grade acetonitrile was purchased from Fisher Chemicals (NJ, USA) and pure water was purchased from Wahaha Co., Ltd., (Hangzhou, Zhejiang Province, China). NADP, glucose-6-phosphate and Tris-HCl buffer were purchased form Sigma, Co., Ltd., (St. Louis, MO, USA). Other reagents (Sodium chloride, Potassium hydroxide, Hydrochloric acid, Dimethyl sulfoxide) were of analytical grade and were purchased from Beijing Fine Chemicals Co., Ltd. (Beijing, China).

Animals

Adult male Sprague-Dawley rats (250–350 g) were bought from the Experimental Animal Center of Peking University Health Science Center. They were handled in accordance with the Guide for the Care and Use of Laboratory Animals of the U.S. National Institutes of Health. The experiments were approved (No. LA2010072) by the Biomedical Ethical Committee of Peking University.

Preparation of rat hepatic S9 fraction

Twenty-four rats were intraperitoneally injected with sodium phenobarbital injection (Tianjin JinYao Amino Acid Co., Ltd., Tianjin, China) at the dosage of 60 $mg \cdot kg^{-1}$ to induce the metabolic enzymes before use. 24 h later, the rats were euthanized by decapitation, and the livers were immediately removed from abdominal cavity, then their wet weights were determined. Subsequently, the livers were minced, and homogenized using a homogenizer (Ultra-Turrax T8, Ika-Werke, Gmbh & Co. KG, Germany) in cold 1.15% KCl in 0.05 $mol \cdot L^{-1}$ Tris-HCl buffer (pH 7.4) to a total volume of 4 × the wet livers weight. The homogenate was centrifuged at 9000 *g* for 30 min under 4 °C condition by a refrigerated centrifuge (Sigma 3K15, SIGMA Laborzentrifugen GmbH, Osterode am Harz, Germany). The 9000 g supernatant (about 1200 mL, 20 mg protein·mL^{-1} determined by Lowry method) as hepatic S9 fraction was obtained and used immediately or temporarily stored at −80 °C for later use in a week [18].

Rat hepatic S9 incubation for metabolite profiling

The general procedure of incubation was depicted in previous report [18]. In brief, 25 ml each of 1.15% KCl, 5 $mmol \cdot L^{-1}$ $MgCl_2$, 5 $mmol \cdot L^{-1}$ glucose-6-phosphate, 0.5 $mmol \cdot L^{-1}$ NADP, and hepatic S9 fraction (20 mg protein per ml) in 0.05 $mol \cdot L^{-1}$ Tris-HCl buffer (pH 7.4) was successively added to a 250 mL flask (on ice) to obtain a reaction system with final volume of 125 mL .

The incubation was conducted in three groups: 1) test group for metabolite profiling, was incubated with 100 mL cofactors, 25 mL hepatic S9 fraction and spiked with 11.25 mg AP (100 μL DMSO solution); 2) control group 1 for excluding endogenous S9 metabolites, was incubated with

100 mL cofactors, 25 ml hepatic S9 and without AP; 3) control group 2 for evaluating the stability of AP, was incubated with 125 mL cofactors (25 ml hepatic S9 was replaced by 25 mL 1.15% KCl in Tris-HCl) spiked with 11.25 mg AP (100 μL DMSO solution).

Afterwards, each flask was incubated in an open-air atmosphere for up to 4 h at 37 °C in a SHA-BA shaker incubator (Hualong instrument Co., Ltd., Jinhua, Zhejiang Province, China), and then 125 mL acetonitrile was added to terminate the reaction. The 250 mL mixture was centrifuged at 3000 r·min^{-1} for 30 min, and the supernatant was evaporated to dry by a rotatory evaporator (Heidolph Laborota 4001, Heidolph Instruments GmbH & Co., Schwabach, Germany) under reduced pressure at 40 °C, and reconstituted to 25 mL with methanol. Then, the samples were stored at −40 °C in an MDF-U5410 Sanyo medical freezer (Sanyo Electric Co., Ltd., Osaka, Japan) before HPLC-DAD-ESI-IT-TOF-MS^n analysis.

Enlarged rat hepatic S9 incubation for isolation of metabolites

The incubation method was the same as that mentioned above. Totally, 450 mg AP was dissolved in 4 mL DMSO and added to 5000 mL reaction mixture (containing 1000 mL rat hepatic S9 fraction), then the mixture was incubated at 37 °C. After 4 h, 5000 mL acetonitrile was added to stop the reaction. The mixture (200 mL or 300 mL each time) was centrifuged at 3000 r·min^{-1} for 30 min, and the supernatant was evaporated under reduced pressure to give a solution (200 mL). The solution was extracted with 200 mL ethyl acetate for four times successively. The combined ethyl acetate solution was evaporated under reduced pressure to give a residue (2.33 g).

All the residue was subjected to D-101 macroporous adsorption resin column chromatography, first eluted with water and then with methanol to give four fractions. Compound 1 (**M1**, 5.3 mg) and compound 2 (**M2**, 6.9 mg) were isolated from fraction 3 by Sephadex LH-20 column chromatography with methanol as eluent, and compound 3 (**M3**, 32.3 mg) and compound 4 (**M4**, 4.7 mg) were isolated from fraction 4 with the same method. Then, each metabolite was purified on a preparative HPLC system (including an Alltech 426 HPLC pump, a UVIS 200 Detector). And the purity of each metabolite was determined to be above 95% by area normalization method at 280 nm with an HPLC-DAD instrument.

HPLC-DAD-ESI-IT-TOF-MS^n analysis

HPLC is a very common technique for qualitative and quantitative analysis of hydrophilic compounds, e.g., monosaccharides produced by bioconversion [19]. However, because the biological samples are very complex and only little structural information can be obtained by HPLC, nowadays tandem techniques are most popular in bioanalysis. For example, an integrated strategy using UPLC-DAD-QTOF-MS for studying the metabolism and pharmacokinetics of herbal medicines has been reported [20]. Accordingly, we also used tandem technique in our research. The resulting samples of test group, control group 1, control group 2, and a reference methanol solution of AP were filtered through 0.45 μm micropore membranes and then analyzed by HPLC-DAD-ESI-IT-TOF-MS^n. The analyses were performed on a Shimadzu LCMS-IT-TOF instrument, which consists of a CBM-20A system controller, two LC-20AD pumps, an SIL-20AC autosampler, a CTO-20A column oven, an SPD-M20A PDA detector, an ESI ion source, and an IT-TOF mass spectrometer.

The HPLC-DAD conditions were as follows: 1) column: Phenomenex Gemini C_{18} (4.6 mm × 250 mm, 5.0 μm); 2) injection volume: 20 μL, column temperature: 35 °C, flow rate: 1.0000 mL·min^{-1}; 3) mobile phase was made up of solvent A (0.1% formic acid solution) and solvent B (acetonitrile); 4) eluent gradient: 0% B for 5 min, 0% B linearly increased to 8% B from 5 min to 15 min, 8% B linearly increased to 25% B from 15 min to 30 min, 25% B linearly increased to 60% B from 30 min to 65 min, 60% B linearly increased to 100% B from 65 min to 80 min, 100% B for 10 min; 5) UV and visible light spectra were obtained by scanning from 200 to 700 nm; 6) HPLC chromatograms were recorded at 210 nm, 254 nm and 280 nm simultaneously.

The ESI-IT-TOF-MS^n parameters were set as follows: 1) flow rate: 0.2000 mL·min^{-1} (split from HPLC effluent); 2) detected in alternating positive ion (PI) and negative ion (NI) mode; 3) ion source temperature: 250 °C; curved desolvation line temperature: 250 °C; ESI nebulization gas flow (Nitrogen): 1.5 L·min^{-1}; ESI interface voltage: (+), 4.5 kV, (−), −3.5kV; detector voltage: 1.80 kV; ion accumulation time: 20 ms; relative collision energy: 50%; 4) mass range: *m/z* 220–1000 in MS, *m/z* 50–1000 in MS^2 and MS^3; 5) A data-dependent program was used in analysis so that the two most abundant ions in each scan were selected and subjected to MS^2 and MS^3 analyses; 6) All data were acquired and processed by Shimadzu LCMS solution Version 3.36, Formula Predictor Version 1.01, and Accurate Mass Calculator software; 7) Mass calibration was carried out using a trifluoroacetic acid sodium solution (2.5 mmol·L^{-1}) from 50 to 1000 Da.

The method for screening the hepatic S9 metabolites of AP and elucidating their structures

Firstly, the chromatographic peaks of probable metabolites were found by comparing the HPLC chromatograms and MS base peak chromatograms (BPCs) of control group 1, control group 2 and test group samples obtained through HPLC-DAD-ESI-IT-TOF-MS^n analysis.

Secondly, the existence of probable metabolites in test group samples was confirmed by comparing the corresponding extracted ion chromatograms (EICs) of two control groups and test group samples.

Thirdly, the conjugation types of phase II metabolites were judged by characteristic neutral losses in MS^2 spectra. For examples, the loss of 176.03 Da ($C_6H_8O_6$), 79.95 Da (SO_3), 162.05 Da ($C_6H_{10}O_5$), and 132.04 Da ($C_5H_8O_4$) indicated that the metabolite was a glucuronide, a sulfate, a hexoside, and a pentoside, respectively.

Fourthly, several (1–3 usually) probable molecular formulae of a metabolite were generated based on MS data by

the Formula Predictor software.

Fifthly, the most probable molecular formula of a metabolite was chosen from the above-mentioned 1–3 probable molecular formulae based on the accurate mass difference between the metabolite and the parent compound and the knowledge of drug metabolism pathways.

Finally, the MS^2 and MS^3 spectra of a metabolite were analyzed to construct the exact structure, and when possible, by direct comparison with the data of standard compounds and the data in the literature.

Spectroscopic Methods

UV spectra (200–400 nm) were recorded by an LCMS-IT-TOF instrument with a DAD detector. HRMS data were obtained by the LCMS-IT-TOF instrument with a TOF mass analyzer or a Bruker Apex IV FT-MS (7.0T). One- and two-dimensional NMR spectra were obtained on a Bruker DRX 400 spectrometer with a 5 mm probe at room temperature. Compounds 1–4 (**M1**–**M4**) were dissolved in 0.5 ml dimethyl sulfoxide-d_6 (DMSO-d_6) containing tetramethylsilane (TMS) as an internal standard. Chemical shifts (δ) were reported in ppm and coupling constants (*J*) in Hertz.

Results

Isolation and structure elucidation of AP metabolites

By means of chromatographic methods, four compounds (**M1**–**M4**) were isolated from rat hepatic S9 mixtures incubated with AP. Their NMR data are summarized in Table 1, and $LCMS^n$ data are shown in Table 2. Their structures are shown in Fig. 1.

M1

M1 was obtained as a white powder, and it showed $[M - H]^-$ at *m/z* 315.0870 in NI mass spectrum and $[M + H]^+$ at *m/z* 317.1001 in PI mass spectrum, indicating that its molecular formula was $C_{17}H_{16}O_6$. The molecular formula had one more oxygen atom than that of AP, suggesting that **M1** was a monohydroxylated metabolite.

Table 1 The ^{1}H NMR (400MHz) and ^{13}C NMR (100MHz) data (measured in DMSO-d_6, δ in ppm, *J* in Hz) of M1–M4 isolated from the rat hepatic S9 incubated with astrapterocarpan

No.	M1		M2		M3		No.	M4	
	δ_C	δ_H (*J*)	δ_C	δ_H (*J*)	δ_C	δ_H (*J*)		δ_C	δ_H (*J*)
1	132.7	7.26 (1H, d, 8.4)	145.6	6.74 (1H, d, 10)	132.6	7.27 (1H, d, 8.4)	1	–	–
2	110.5	6.44 (1H, dd, 8.4, 2.4)	128.4	6.05 (1H, dd, 1.6, 10)	110.1	6.33 (1H, d, 7.6)	2	65.7	4.24 (2H, br.)
3	156.0	–	186.9	–	156.8	–	3	35.4	3.44 (1H, d, 3.6)
4	103.1	6.20 (1H, d, 2.4)	106.2	5.34 (1H, d, 1.6)	103.2	6.26 (1H)	4	75.2	4.28 (1H, d, 3.6)
5	–	–	–	–	–	–	5	132.1	7.00 (1H, d, 8.4)
6	69.6	3.92 (2H, dd, 11.6, 11.2)	66.8	4.95 (1H, dd, 3.2, 10.8); 4.37 (1H, d, 10.8)	66.3	4.18 (1H, d, 6.8) 3.57 (1H, d, 6.8)	6	108.6	6.29 (1H, dd, 2.4, 8.4)
7	106.0	6.58 (1H, d, 8.4)	106.0	6.96 (1H, d, 8.4)	109.0	6.46 (1H, d, 7.6)	7	155.6	9.39 (1H, s, OH)
8	118.3	7.00 (1H, d, 8)	118.9	6.52 (1H, d, 8.4)	119.9	6.80 (1H, d, 7.6)	8	102.6	6.16 (1H, d, 2.4)
9	151.6	–	151.9	–	150.7	–	9	158.7	–
10	133.8	–	132.8	–	132.9	–	10	112.8	–
4a	159.5	–	171.0	–	159.2	–	1′	119.9	–
1a	111.5	–	67.4		111.7	–	2′	152.1	8.99 (1H, s, OH)
11a	85.2	5.22 (1H, s)	83.4	5.20 (1H, d, 10)	78.9	5.50 (1H, d, 6.4)	3′	136.4	–
6a	75.6	–	40.0	4.05 (1H, d, 10)	40.0	3.55 (1H, br.)	4′	148.4	–
7a	124.8	–	121.3		119.2	–	5′	103.5	6.31 (1H, d, 8.4)
10a	153.9	–	152.9	–	151.6	–	6′	122.3	6.64 (1H, d, 8.8)
9-OCH_3	56.7	3.73 (3H, s)	56.6	3.70 (3H, s)	–	–	4-OCH_3	55.4	3.29 (3H, s)
10-OCH_3	60.4	3.68 (3H, s)	60.0	3.50 (3H, s)	60.2	3.7 (3H, s)	3′-OCH_3	60.7	3.65 (3H, s)
							4′-OCH_3	56.0	3.68 (3H, s)

In the ^{1}H NMR spectrum, the signal assigned to H-6a was not observed at δ 4.22 (1H, d, *J* = 5.6Hz) in contrast to that of AP. ^{13}C NMR spectrum of **M1** exhibited a C-6a signal at δ 75.6, which was shifted downfield compared with that of C-6a at δ 40.0 in AP, suggesting that the newly added hydroxyl group was linked to C-6a. Its location was further deduced to be at C-6a from the correlations of H-11a (δ 5.22, 1H, s) and H-6 (δ 3.92, 2H, dd, *J* = 11.6, 11.2 Hz) to C-6a in the HMBC spectrum. Meanwhile, the signals of C-6 and C-11a had shifted downfield from δ 66.1 to δ 69.6 and from δ 79.0 to δ 85.2, respectively, in comparison with that of AP. Thus, **M1** was named as 6a-hydroxy-AP. It was a new compound and a new metabolite of AP.

Table 2 HPLC-DAD-ESI-IT-TOF-MS^n data of astrapterocarpan (AP) and its 40 metabolites formed in rat hepatic S9

No.	t_R (min)	Meas. (Da)[a]	Pred. (Da)[a]	Error[a] (ppm)	Characteristic fragment ions[a]	Formula	UV λ_{max} (nm)	Peak area%[c]	Metabolic reactions
AP	50.263	301.1075	301.1071	1.33	MS^2: 167.0720; 191.0709; 147.0432; 163.0408; 207.0642; 123.0441; 179.0720 MS^3(167.0719): 152.0470; 134.0345; 139.0724; 124.0539; 106.0410; 96.0548	$C_{17}H_{16}O_5$	220, 282	–	parent compound
M1	39.760	317.1001	317.1020	–5.99	MS^2(299.0898): 147.0433; 137.0539; 155.0701; 134.0341; 284.0671; 266.0562; 238.0616	$C_{17}H_{16}O_6$	207, 234, 280	0.83	+O at 6a
M2	38.267	317.1024	317.1020	1.26	MS^2: 299.0859; 139.0362; 191.0696; 167.0692; 176.0459; 163.0418; 179.0328; 207.0655	$C_{17}H_{16}O_6$	208, 231, 285, 307	14.01	+O at 1a and rearrangement
M3	44.445	287.0926	287.0914	4.18	MS^3(287.0915): 147.0430; 153.0526; 177.0542; 193.0459; 163.0373; 165.0558; 123.0436	$C_{16}H_{14}O_5$	220, 282	11.49	$-CH_2$ at 9-OCH_3
M5	32.003	303.0864	303.0863	0.33	MS^2: 139.0371; 177.0548; 153.0542; 163.0397; 179.0296 MS^3(177.0547): 121.0654; 162.0290; 91.0488	$C_{16}H_{14}O_6$	237, 285, 308	2.15	+O on A/C-ring; $-CH_2$
M6	32.427	333.0967	333.0969	–0.60	MS^2: 179.0332; 183.0658; 167.0688; 151.0386; 181.0474	$C_{17}H_{16}O_7$	238, 284, 306	2.52	+O on A/C-ring; +O on B-ring
M7[b]	33.332	301.0722	301.0718	1.33	MS^2: 286.0455; 257.0835; 242.0538; 191.0357; 176.0137	$C_{16}H_{14}O_6$	208, 234, 280	0.42	+O at 1/2/4/6/11a; $-CH_2$
M8	33.435	317.1011	317.1020	–2.84	MS^2: 167.0697; 139.0379; 163.0416; 191.0580 MS^3(167.0697): 152.0400; 134.0332; 106.0300	$C_{17}H_{16}O_6$	241, 279	0.47	+O on A-ring
M9	33.685	303.0845	303.0863	–5.94	MS^2: 177.0555; 153.0543; 139.0358; 149.0635	$C_{16}H_{14}O_6$	245, 309	0.25	+O on A-ring; $-CH_2$
M10[b]	34.117	331.0819	331.0823	–1.21	MS^2: 289.0722; 207.0672; 177.196; 192.0494 MS^3(289.0723): 153.0590; 138.0305; 123.0097; 230.0630	$C_{17}H_{16}O_7$	239, 278	1.11	+O on A-ring; +O on B-ring
M11[b]	34.858	331.0813	331.0823	–3.02	MS^2: 316.0515; 313.0740; 289.0699; 271.0590; 256.0270 MS^3(289.0700): 274.0491; 259.0231; 227.0340	$C_{17}H_{16}O_7$	246, 291	0.63	+O on A-ring; +O at 6
M12[b]	35.548	301.0711	301.0718	–2.33	MS^2: 286.0442; 271.0643; 268.0414; 256.0385; 164.0157 MS^3(256.0385): 183.0416; 200.0651; 211.0398; 227.0317; 238.0282(25.07); 239.0245	$C_{16}H_{14}O_6$	250, 282, 300	0.45	+O on A/C-ring; $-CH_2$
M13	36.048	317.1014	317.1020	–1.89	MS^2: 167.0708; 191.0652; 122.0506; 147.0798; 163.0362	$C_{17}H_{16}O_6$	251, 279	0.04	+O on A-ring
M14	36.947	319.1159	319.1176	–5.33	MS^2: 135.0411; 140.0463; 147.0460; 155.0761; 167.0691; 289.1032; 301.0975 MS^3(167.0691): 94.0398; 106.0400; 134.0376; 152.0520	$C_{17}H_{18}O_6$	242, 283	0.58	+H_2O on D-ring
M15	37.403	303.0857	303.0863	–5.94	MS^2: 177.0539; 153.0533; 139.0372; 163.0362	$C_{16}H_{14}O_6$	239, 279	0.38	+O on A/C-ring
M16	37.662	273.0769	273.0758	4.03	MS2: 123.0388; 139.0391; 147.0448; 163.0386; 245.0754 MS^3(139.0391): 111.0399	$C_{15}H_{12}O_5$	247, 278	0.36	$-2CH_2$
M17	38.802	303.0861	303.0863	–0.66	MS^2: 153.0532; 285.0720; 177.0524; 139.0354; 163.0379; 179.0308; 193.0482 MS^3(153.0532): 138.0298; 125.0649; 107.0474; 93.0307; 77.0326	$C_{16}H_{14}O_6$	204, 232, 292	8.35	+O at 1/2/4/6/11a; $-CH_2$
M18	39.302	479.1530	479.1548	–3.76	MS^2: 317.1010 MS^3(317.1010): 191.0580; 167.0684	$C_{23}H_{26}O_{11}$	251, 279	0.05	+O on A-ring; +Glc
M19	39.423	463.1597	463.1599	–0.43	MS^2(301.1061): 147.0417; 167.0704; 191.0647 MS^3(167.0703): 134.0376; 139.0786	$C_{23}H_{26}O_{10}$	238, 280	0.65	+Glc at 3-OH
M20	40.192	303.0861	303.0863	–0.66	MS^2: 285.0638; 193.0449; 177.0541; 163.0386; 153.0535 MS^3(153.0535): 138.0280; 125.0556	$C_{16}H_{14}O_6$	242, 295	1.77	+O at 1/2/4/6/11a; $-CH_2$
M21	41.443	333.0951	333.0969	–5.40	MS^2: 151.0383; 179.0324; 167.0701; 181.0787	$C_{17}H_{16}O_7$	251, 279	0.04	+O on A-ring; +O on B-ring
M22	41.745	317.1006	317.1020	–4.42	MS^2: 179.0344; 167.0680; 163.0362; 207.0590; 191.0666	$C_{17}H_{16}O_6$	251, 279	0.05	+O on A-ring
M23	42.022	301.0698	301.0707	–2.99	MS^2: 163.0362; 241.0439; 245.0799; 269.0527; 273.0718; 283.0625 MS^3(245.0799): 123.0423; 185.0578; 213.0499; 229.0477; 230.0409	$C_{16}H_{12}O_6$	252, 305, 340	1.35	+O on A-ring; $-CH_2$; −2H of C6–C6a

Continued

No.	t_R (min)	Meas. (Da)[a]	Pred. (Da)[a]	Error[a] (ppm)	Characteristic fragment ions[a]	Formula	UV λ_{max} (nm)	Peak area%[c]	Metabolic reactions
M24	42.755	317.1014	317.1020	–1.89	MS^2: 299.0920; 167.0711; 183.0689; 163.0486 MS^3(299.0919): 238.0626; 257.0674; 266.0694; 284.0653 MS^2(299.0896): 284.0661; 266.0580; 238.0583; 134.0284	$C_{17}H_{16}O_6$	251, 279	0.05	+O at 6a
M25	43.842	317.1014	317.1020	–1.89	MS^2: 299.0933; 167.0695; 139.0387; 191.0706; 163.0404; 179.0338; 207.0630	$C_{17}H_{16}O_6$	219, 278	19.62	+O at 6
M26	45.048	317.1015	317.1020	–1.58	MS^2: 167.0692; 207.0640; 191.0709; 163.0374; 179.0345; 299.0919; 139.0376	$C_{17}H_{16}O_6$	205, 232, 293	14.10	+O at 6
M27	46.075	317.1017	317.1020	–0.95	MS^2: 299.0921; 167.0708; 179.0663; 163.0392; 183.0657; 207.0671; 155.0666; 123.0437; 111.0540; 140.0450	$C_{17}H_{16}O_6$	277, 313	1.73	+O at 6a with rearranged-A ring
M28	49.425	315.0861	315.0863	–0.63	MS^2: 299.0517; 297.0769; 287.0885; 259.0955; 149.0223 MS^3(259.0956): 243.0686; 227.0714; 212.0455; 197.0517; 137.0592; 123.0411; 105.0431	$C_{17}H_{14}O_6$	252, 340	2.59	+O on A-ring; −2H of C6–C6a
M29	50.607	301.0718	301.0707	3.65	MS^2: 286.0449; 283.0522; 273.0776; 245.0754; 241.0494; 213.0561 MS^3(286.0449): 150.0247; 137.0225	$C_{16}H_{12}O_6$	247, 334, 347	0.48	+O on A-ring; $-CH_2$; −2H of C6a–C11a
M30	52.807	615.1843	615.1861	–2.93	MS^2: 283.0611; 419.0992; 437.1205; 461.1128 MS^3(437.1207): 255.0643; 283.0589; 419.1032	$C_{34}H_{30}O_{11}$	251, 282	0.27	Dimerization (A-ring↔A′-ring); +O on A-ring
M31	53.600	571.1588	571.1599	–1.93	MS^2: 407.1126 MS^3(407.1126): 147.0445; 213.0499; 227.0246; 261.0761; 389.0755	$C_{32}H_{26}O_{10}$	251, 283	0.68	Dimerization (A-ring↔A′-ring); $-2CH_2$ (B-ring, B′-ring)
M32	55.413	615.1857	615.1861	–0.65	MS^2: 283.0597; 437.1251; 461.1161 MS^3(461.1161): 179.0734; 283.0565	$C_{34}H_{30}O_{11}$	252, 283	0.27	Dimerization (A-ring↔A′-ring); +O on A-ring
M33	56.802	571.1588	571.1599	–1.93	MS^2: 461.1122; 449.1150; 437.1180; 419.1092; 313.0734; 285.0638 MS^3(461.1121): 429.0904	$C_{32}H_{26}O_{10}$	252, 286	0.46	Dimerization (A-ring↔C′-ring); $-2CH_2$ (B-ring, B′-ring)
M34	58.072	585.1755	585.1755	0.00	MS^2: 445.1265; 431.1193; 421.1275; 407.1146 MS^3(421.1275): 299.0845; 269.0761; 255.0617; 243.0652; 239.0654; 215.0672; 191.0692; 167.0687	$C_{33}H_{28}O_{10}$	248, 284	2.61	Dimerization (A-ring↔A′-ring); $-CH_2$
M35	58.563	585.1744	585.1755	–1.88	MS^2: 476.1524; 431.1128; 421.1179; 407.1122; 343.1370	$C_{33}H_{28}O_{10}$	247, 285	0.14	Dimerization (A-ring↔C′-ring); $-CH_2$
M36	59.563	599.1901	599.1912	–1.84	MS^2: 584.1696; 421.1273 MS^3(421.1273): 243.0641; 225.0552; 267.0665; 239.0679; 207.0590	$C_{34}H_{30}O_{10}$	247, 282	2.40	Dimerization (A-ring↔A′-ring)
M37	61.168	585.1745	585.1755	–1.71	MS^2: 445.1265; 407.1085; 405.0936; 299.0924; 241.0363	$C_{33}H_{28}O_{10}$	253, 285	0.29	Dimerization (A-ring↔A′-ring); $-CH_2$
M38	61.747	585.1748	585.1755	–1.20	MS^2: 475.1289; 463.1433; 431.1121; 407.1134; 297.0653; 285.0802; 191.0688 MS^3(407.1134): 347.0757; 297.0820	$C_{33}H_{28}O_{10}$	252, 285	1.31	Dimerization (A-ring↔C′-ring); $-CH_2$
M39	63.125	599.1912	599.1912	0.00	MS^2: 583.1597; 445.1288; 431.1153; 421.1277 MS^3(421.1277): 243.0631; 215.0673; 267.0649; 239.0686; 255.0631; 299.0923; 191.0668; 167.0690	$C_{34}H_{30}O_{10}$	239, 284	4.96	Dimerization (A-ring↔A′-ring)
M40	63.478	615.1835	615.1861	–4.23	MS^2: 461.1337; 437.1202; 303.0828; 284.0998; 253.0691 MS^3(284.0998): 269.0821; 267.0966	$C_{34}H_{30}O_{11}$	252, 282	0.08	Dimerization (A-ring↔A′-ring); +O on A-ring
M41	64.297	585.1763	585.1755	1.37	MS^2: 463.1437; 407.1134; 391.1231; 299.0859; 297.0820; 285.0738 MS^3(407.1134): 297.0740; 177.0534	$C_{33}H_{28}O_{10}$	254, 283	0.05	Dimerization (A-ring↔C′-ring); $-CH_2$

Note: t_R, retention time; +O, hydroxylation; $-CH_2$, demethylation; −2H, dehydrogenation; −, not calculated.

[a] Detected under positive ion mode.

[b] Detected under negative ion mode.

[c] The value was calculated as: (peak area of each metabolite) / (total peak area of 40 metabolites) × 100 %, and the peak area was determined from base peak chromatogram in negative ion mode.

M2

M2 was obtained as a yellow powder, and it showed $[M-H]^-$ at *m/z* 315.0872 and $[M+H]^+$ at *m/z* 317.1024, indicating that its molecular formula was also $C_{17}H_{16}O_6$. The molecular formula had one more oxygen atom than that of AP, suggesting that **M2** was also a monohydroxylated metabolite.

The ^{1}H NMR of **M2** showed H-1 (δ 6.74, 1H, d, *J* = 10 Hz), H-2 (δ 6.05, 1H, dd, *J* = 1.6, 10 Hz), H-4 (δ 5.34, 1H, d, *J* = 1.6 Hz), H-6_{eq} (δ 4.95, 1H, dd, *J* = 3.2, 10.8 Hz), H-6_{ax} (δ 4.37, 1H, d, *J* = 10.8Hz), H-6a (δ 4.05, 1H, d, *J* = 10 Hz), H-11a (δ 5.20, 1H, d, *J* = 10Hz), H-7 (δ 6.96, 1H, d, *J* = 8.4 Hz), H-8 (δ 6.52, 1H, d, *J* = 8.4 Hz), 9-OCH_3 (δ 3.70, 3H, s), 10-OCH_3 (δ 3.50, 3H, s), which were similar to those of 1a-hydroxy-9-methoxy-pterocarp-1(2), 4-diene-3-one [21], suggesting that **M2** had a rearrangement structure in A-ring and a hydroxy at C-1a.

The ^{1}H and ^{13}C NMR and HMQC spectrum displayed two methyls, nine methines, and six quaternary carbons (one ketone carbonyl, four oxygenated, one olefinic carbon). In the HMBC experiment, H-1 (δ 6.74, 1H, d, *J* = 10 Hz) correlated with C-4a (δ 171.0) and C-3 (δ 186.9), H-6_{eq} (δ 4.95, 1H, dd, *J* = 3.2, 10.8 Hz) correlated with C-11a (δ 83.3), C-7a (δ 121.3) and C-4a (δ 171.0), H-6_{ax} (δ 4.37, 1H, d, *J* = 10.8Hz) correlated with C-4a (δ 171.0), C-11a (δ 83.3) and C-7a (δ 121.3), H-6a (δ 4.05, 1H, d, *J* = 10Hz) correlated with C-7a (δ 121.3) and C-6 (δ 66.83), and H-11a (δ 5.20, 1H, d, *J* = 10Hz) correlated with C-6 (δ 66.8) and C-4a (δ 171.0). Meanwhile, the signals of C-1, C-2, and C-4 had shifted downfield from δ 132.6 to 145.6, from δ 110.2 to 128.3, and from δ 103.2 to 106.2, respectively, in comparison with that of AP, which further indicated that **M2** had a rearrangement structure in A ring and a hydroxy at C-1a. Thus, **M2** was named as astrametabolin I [1a-hydroxy-9, 10-dimethoxy-pterocarp-1(2), 4-diene-3-one]. **M2** was a new compound and a new metabolite of AP.

M3

M3 was obtained as a white powder, and it showed $[M-H]^-$ at *m/z* 285.0767 and $[M+H]^+$ at 287.0926, indicating that its molecular formula was $C_{16}H_{14}O_5$. The molecular formula had one less methylene than that of AP, suggesting that **M3** was a demethylated metabolite of AP.

The ^{13}C NMR spectrum of **M3** revealed 16 carbon signals, and had one less methyl signal at δ 56.0 (C-9) in contrast to that of AP, suggesting that the demethylation occurred at the methoxyl group linked to C-9. The structure of **M3** was elucidated as 9-demethyl-AP (nissolin) by comparing its spectra data with those of 9-demethyl-AP in the literature [3]. **M3** was a new metabolite of AP.

M4

M4 was obtained as a white powder, and it showed $[M-H]^-$ at *m/z* 331.1186 in NI mass spectrum of HR-ESI-FT-MS, so its molecular formula was determined to be $C_{18}H_{20}O_6$.

The ^{1}H and ^{13}C NMR (Table 1) and HMQC spectra showed three methyls, one methylene, seven methines (one oxygenated), seven quaternary carbons (five oxygenated, two olefinic carbons). In the HMBC spectrum, H-2 (δ 4.24, 2H, br.) correlated with C-1′ (δ 120.0) and C-9 (δ 158.7), H-5 (δ 7.00, 1H, d, *J* = 8.4 Hz) correlated with C-7 (δ 155.6), C-4 (δ 75.2) and C-9 (δ 158.7), H-8 (δ 6.16, 1H, d, *J* = 2.4Hz) correlated with C-7 (δ 155.6), C-10 (δ 112.8) and C-9 (δ 108.6), and H-6′ (δ 6.64, 1H, d, *J* = 8.8 Hz) correlated with C-4′ (δ 148.4) and C-2′ (δ 152.1), and ^{1}H NMR spectrum showed an additional signal at δ 3.29 (3H, s), and ^{13}C NMR spectrum showed one more signal at δ 55.5 of methoxy in contrast to that of astraisoflavan [22]. Meanwhile, the signals of C-4 had shifted downfield from δ 31.3 to 75.2, suggesting that **M4** was a methoxylation product of astraisoflavan, and the position was at C-4. Thus, **M4** was named as 4-methoxy-astraisoflavan (7, 2′-dihydroxy-4, 3′, 4′-trimethoxy-isoflavan). **M4** was a new compound and a new degradation product of AP.

Metabolite profiling of AP in rat hepatic S9 by HPLC-DAD-ESI-IT-TOF-MS^n analysis

The metabolites of AP produced in rat hepatic S9 fraction were analyzed by HPLC-DAD-ESI-IT-TOF-MS^n technique. And totally 40 new metabolites of AP were found and tentatively identified.

The representative BPCs of the test group, control group 1, control group 2 and AP reference standard in NI mode are shown in Fig. 2. The identified metabolites were labeled with **M1**–**M41**, and their HPLC-DAD-ESI-IT-TOF-MS^n data are summarized in Table 2.

The MS^n fragmentation behavior of AP

To facilitate the metabolite structure identification, the MS^n fragmentation behavior of parent compound AP in PI mode and NI mode was firstly studied. As a result, we found that the fragmentation behavior in PI mode can provide more information about the structures. Therefore, the metabolite structure elucidation was mostly by PI mass spectra data. The nomenclature for fragmentations of pterocarpans in PI mode was partly adopted from literature [23] and is shown in Fig. 3.

AP had a retention time of 50.263 min. Its UV spectrum showed maximum absorption at 220, 282 nm. It showed $[M+H]^+$ at *m/z* 301.1075 in PI mass spectrum and $[M-H]^-$ at *m/z* 299.0924 in NI mass spectrum. So, its molecular formula was determined to be $C_{17}H_{16}O_5$. In MS^2 PI mass spectrum, it showed a base peak ion at *m/z* 167.0720 ($^{2,3,5}B^+ + H$) and many other characteristic fragment ions ($^{1,4}B^+ - 2H$, $^{5,6}A^+ - 2H$, $^{6,7}A^+ - 2H$, $^{0,4}B^+ - 2H$, $^{1,3,5}A^+ + H$, $^{2,4}B^+$, $^{3,4,6}A^+ - 2H$). Based on MS^2 and MS^3 data, its major fragmentation pathways in PI mode were proposed and are shown in Fig. 4.

Monohydroxylated metabolites-M1, M2, M8, M13, M22, M24, M25, M26, M27

Nine monohydroxylated metabolites were identified; they were **M1**, **M2**, **M8**, **M13**, **M22**, **M24**, **M25**, **M26**, and **M27**. The retention times, characteristic MS^n fragment ions and UV maximum absorption wavelength of them are summarized in Table 2. All of them showed $[M+H]^+$ at *m/z* 317.10 in PI mass spectrum and $[M-H]^-$ at *m/z* 315.08 in NI mass spectrum, and their molecular formulae were predicted to be $C_{17}H_{16}O_6$.

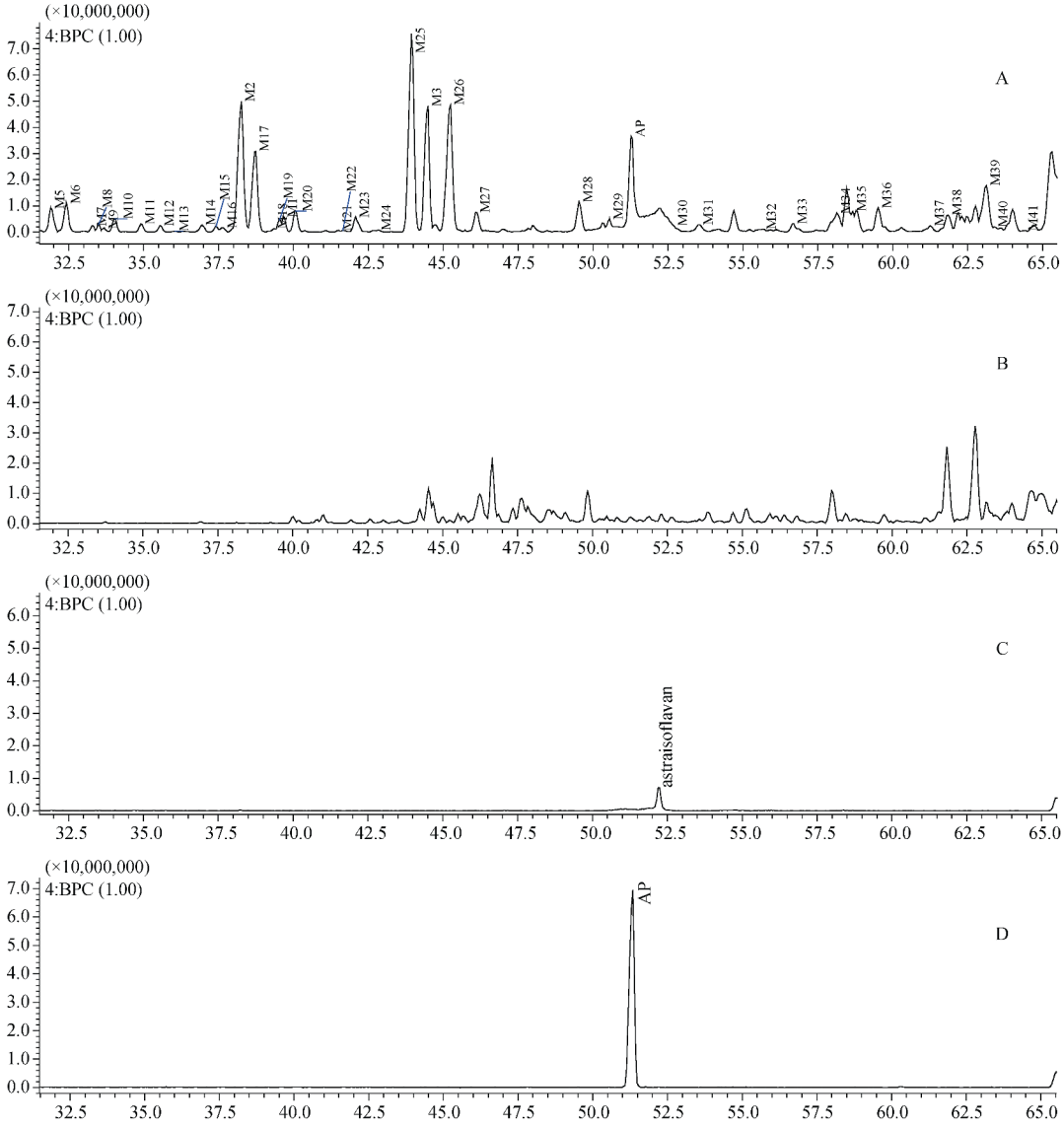

Fig. 2 Representative negative ion base peak chromatograms of the samples in rat hepatic S9 incubation experiment. (A) Test group, the sample was incubated with cofactors, hepatic S9 and astrapterocarpan (AP) for 4 h; (B) Control group 1, the sample was incubated with cofactors, hepatic S9 and without AP for 4 h; (C) Control group 2, the sample was incubated with cofactors, AP and without hepatic S9 for 4 h. AP was not stable and could be transformed to astraisoflavan, but no other products could be detected; (D) Reference standard of AP dissolved in methanol. M1–M41 denote metabolites, AP denotes astrapterocarpan

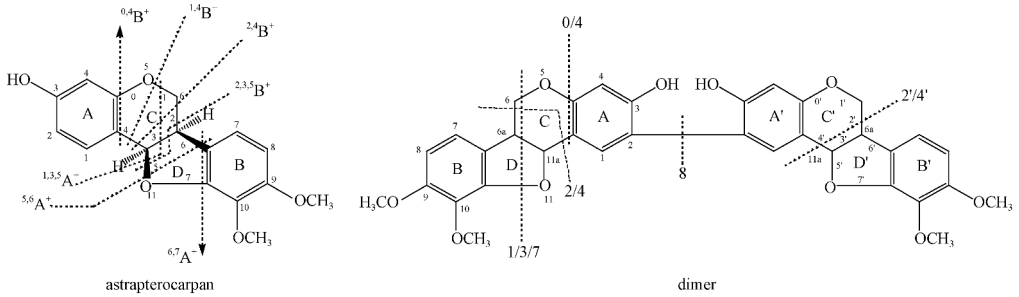

Fig. 3 The atom position numbering and the nomenclature for fragmentations of astrapterocarpan and its dimers. The rings are labeled with capital letters. The italic numbers outside the ring denote the atom position numbering. The bold numbers inside the ring denote the bond numbering. The fragmentations are expressed as bond numbers separated with slashes. For dimers, the left or upper monomer is labeled with numbers or letters, and the right or below monomer is labeled with numbers or letters and a prime symbol

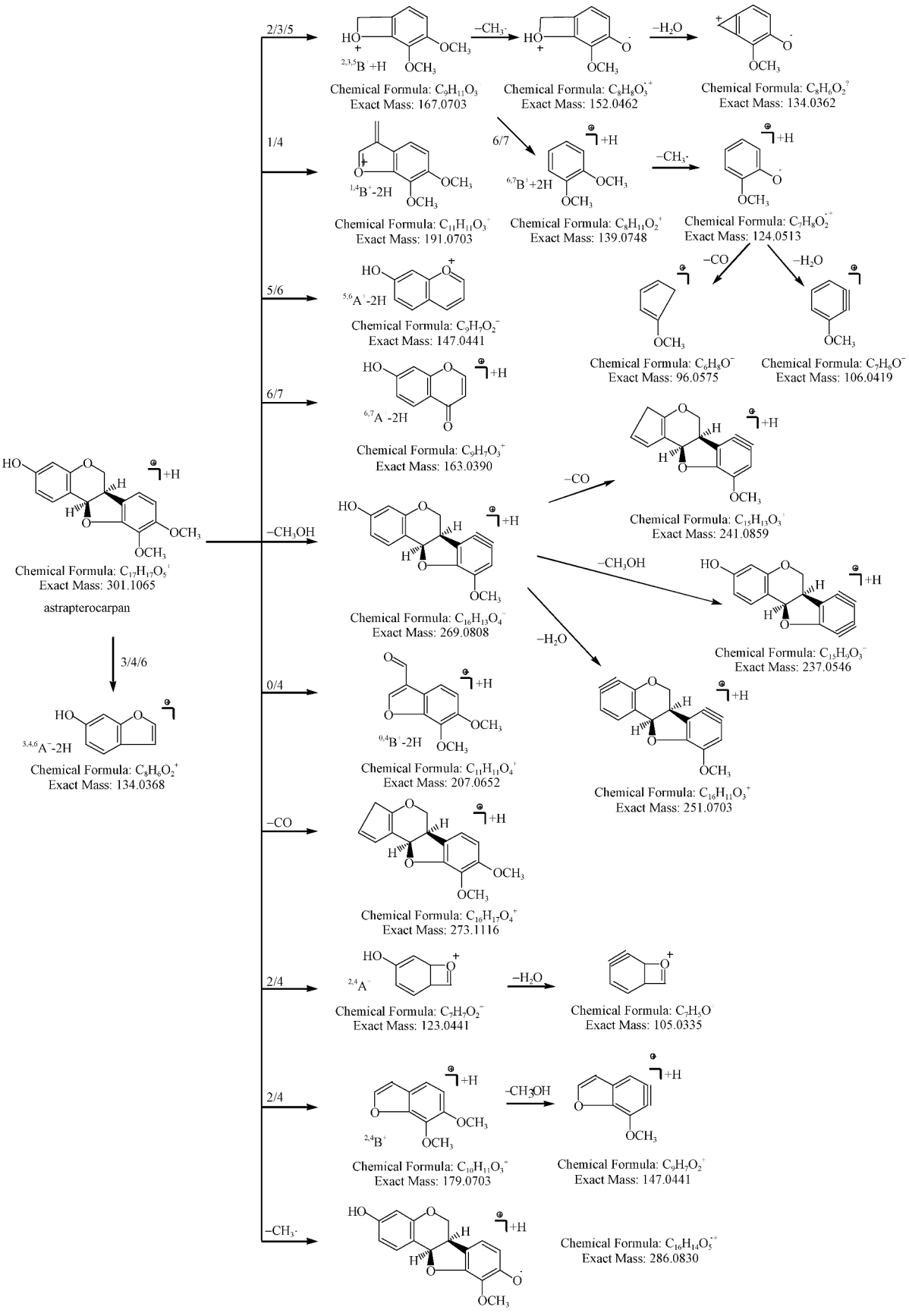

Fig. 4 The proposed fragmentation pathways of astrapterocarpan in positive ion detection mode

M1 and **M2** had been isolated and identified as 6a-hydroxy-AP and astrametabolin I as mentioned in the above section.

After careful analysis of the MS^n data of these metabolites, we ascertained that the monohydroxylation should occur on C ring or A ring, but the exact position could not be determined by current HPLC-MS technique in most situations. Considering there were only 6 sites (carbon position number: 1, 2, 4, 6, 6a, 11a) on C ring and A ring, but 9 monohydroxylation products were observed, we can deduce that some metabolites might have an A ring with the rearrangement structure like that of **M2**, and/or some metabolites might be diastereomers.

M1

M1 had been isolated and identified as 6a-hydroxy-AP as mentioned before. In PI mode, the MS^2 and MS^3 mass spectra of $[M + H]^+$ of **M1** were not obtained, because it was very easy to loss of a H_2O from $[M + H]^+$, suggesting that the monohydroxylation might occur on C ring. In fact, the hydroxyl group was attached to carbon 6a. In NI mode, its $[M - H]^-$ gave a characteristic fragment ion at *m/z* 153.0603 ($^{5,6}B^- + 2H$), which further confirmed that the hydroxylated position must not be on B ring.

M2

M2 had been isolated and identified as astrametabolin I as mentioned before. In its MS^2 PI mass spectrum, the characteristic fragment ions at *m/z* 139.0362, 191.0696, 167.0692, 176.0459, 79.038, 207.0655 and 163.0418 were observed. The existence of these ions indicated that the monohydroxylated position might be on C ring or A ring.

M8

In PI mode, its $[M + H]^+$ can fragment to the product ions at *m/z* 167.0697 ($^{2,3,5}B^+ + H$), 139.0379 ($^{1,3,7}A^+ + H$ or $^{2,4}A^+$), 163.0416 ($-H_2O^{6,7}A^+$ or $^{5,6}A^+ - 2H$), and 191.0580 ($-H_2O^{1,4}B^+$ or $^{1,4}B^+ - 2H$), which suggested that the hydroxylation site might be on A ring or C ring. Besides, no loss of H_2O from $[M + H]^+$ was observed in its MS^2 mass spectrum, which suggested that the hydroxy might not be on C ring. Thus, we tentatively identified M8 as A-ring-monohydroxylated AP.

M13

In MS^2 and MS^3 mass spectra of **M13**, the characteristic fragment ions at *m/z* 167.0708 ($^{2,3,5}B^+ + H$), 191.0652 ($-H_2O^{1,4}B^+$ or $^{1,4}B^+ - 2H$), 163.0362 ($-H_2O^{6,7}A^+$ or $^{5,6}A^+ - 2H$), and 122.0506 ($^{1,3,5}A^+$ or $^{0,3,5}A^+$) were observed, which indicated that the hydroxylation site was on A ring or C ring. Besides, no loss of H_2O from $[M + H]^+$ was observed in its MS^2 mass spectrum, which suggested that the hydroxy might not be on C ring. Therefore, **M13** was also A-ring- monohydroxylated AP.

M22

The fragment ions at *m/z* 179.0344 ($^{6,7}A^+ - 2H$), 167.0680 ($^{2,3,5}B^+ + H$), 163.0362 ($-H_2O^{6,7}A^+$ or $^{5,6}A^+ - 2H$), 207.0590 ($^{1,4}B^+ - 2H$ or $^{0,4}B^+ - 2H$), 191.0666 ($-H_2O^{1,4}B^+$ or $^{1,4}B^+ - 2H$) in MS^2 mass spectrum of **M22** indicated that the newly added hydroxyl group should be attached to A ring or C ring. Besides, there was no fragment ion at *m/z* 299.09 (loss of H_2O from $[M + H]^+$) in its MS^2 mass spectrum, which suggested that the hydroxy might not be on C ring. Thus, we tentatively identified **M22** as A-ring-monohydroxylated AP.

M24

In the MS^2 PI mass spectrum of **M24**, the base peak ion was *m/z* 299.0920, which implied that it was easy to loss a H_2O from **M24**, and the newly added hydroxy might be linked to C ring. The fragment ions at *m/z* 183.0689 ($^{2,3,5}B^+ + H$), 163.0486($-H_2O^{6,7}A^+$ or $^{5,6}A^+ - 2H$) indicated that the hydroxy should be linked to carbon 6a. Besides, the MS^2 spectrum of $[M - H_2O + H]^+$ was similar to that of **M1**. Therefore, **M24** might be a diastereomer of **M1**, and the newly added hydroxy was on C ring at carbon 6a. It was 6a-hydroxy-AP isomer.

M25

In the MS^2 PI mass spectrum of **M25**, the fragment ions at *m/z* 167.0695 ($^{2,3,5}B^+ + H$), 139.0387 ($^{2,4}A^+$ or $^{1,3,7}A^+ + H$), 191.0706 ($- H_2O^{1,4}B^+$), 163.0374 ($- H_2O^{6,7}A^+$ or $^{5,6}A^+ - 2H$), 179.0338 ($^{6,7}A^+ - 2H$), and 207.0640 ($^{1,4}B^+ - 2H$) indicated that the newly added hydroxy might be linked to A ring or C ring (carbon 6 or 11a). Besides, there was a fragment ion at *m/z* 299.09 (loss of H_2O from $[M + H]^+$) in its MS^2 mass spectrum, which suggested that the hydroxy might be on C ring. As a result, we tentatively identified **M25** as 6-hydroxy-AP.

M26

In the MS^2 PI mass spectrum of **M26**, the fragment ions at *m/z* 167.0692 ($^{2,3,5}B^+ + H$), 139.0376 ($^{2,4}A^+$ or $^{1,3,7}A^+ + H$), 191.0709 ($- H_2O^{1,4}B^+$), 163.0404 ($- H_2O^{6,7}A^+$ or $^{5,6}A^+ - 2H$), 179.0345 ($^{6,7}A^+ - 2H$), and 207.0630 ($^{1,4}B^+ - 2H$) indicated that the newly added hydroxy might be linked to C ring (carbon 6 or 11a) or A ring. Besides, there was a fragment ion at *m/z* 299.09 (loss of H_2O from $[M + H]^+$) in its MS^2 mass spectrum, which suggested that the hydroxy might be on C ring. As a result, we tentatively identified **M26** as a diastereomer of **M25**, i.e., 6-hydroxy-AP isomer.

M27

In the MS^2 PI mass spectrum of **M27**, the fragment ions at *m/z* 299.0921, 167.0708 ($- H_2O^{2,3,5}B^+ + 2H$), 179.0663 ($^{1,3,5}B^+ + H$), 163.0392 ($- H_2O^{6,7}A^+$ or $^{5,6}A^+ - 2H$), 183.0657 ($^{2,3,5}B^+ + H$), 207.0671 ($^{1,4}B^+ - 2H$), 155.0666 ($^{5,6}B^+ + 2H$), 123.0437 ($^{2,4}A^+$), 111.0540 ($^{1,4}A^+ + 2H$), and 140.0450 ($^{1,3,7}B^+ + 2H$) indicated that the newly added hydroxy might be linked to carbon 6a on C ring. **M27** might be an isomer of **M1**, perhaps with a rearranged A-ring.

Demethylated metabolite-M3

M3 had been isolated and identified to be 9-demethyl-AP as mentioned before. In the MS^3 mass spectrum of *m/z* 287.0915, the fragment ions at 147.0430 ($^{5,6}A^+ - 2H$), 153.0526 ($^{2,3,5}B^+ + H$), 177.0542 ($^{1,4}B^+ - 2H$), 193.0459 ($^{0,4}B^+ - 2H$), 163.0373 ($^{6,7}A^+ - 2H$), 165.0558($^{2,4}B^+$), and 123.0436 ($^{2,4}A^+$ or $^{1,3,5}A^+ + H$) were observed. The masses of

the fragment ions containing B-ring all were 16 Da less than those of the corresponding fragment ions from the parent compound, indicating demethylation on B-ring.

Demethylated and monohydroxylated metabolites-M5, M7, M9, M12, M15, M17, M20

All of these metabolites showed $[M + H]^+$ at *m/z* 303.08 in PI mass spectrum and $[M - H]^-$ at *m/z* 301.07 in NI mass spectrum. Based on the exact masses of the ions, their molecular formula were determined to be $C_{16}H_{14}O_6$, suggesting that they were demethylation and monohydroxylation products of AP.

M5

The fragment ions at *m/z* 177.0548 ($^{1,\ 4}B^+ - 2H$), 153.0542 ($^{2,\ 3,\ 5}B^+ + H$ or $^{3,\ 4,\ 6}A^+ + H$), 139.0371 ($^{2,\ 4}A^+$ or $^{5,\ 6}B^+$ or $^{1,\ 3,\ 5}A^+ + H$), 163.0397 ($^{5,\ 6}A^+ - 2H$ or $^{2,\ 4}B^+ - 2H$), 179.0296 ($^{6,\ 7}A^+ - 2H$) in the MS^2 PI mass spectrum of **M5** indicated that the newly added hydroxy might be attached to A ring or C ring. Accordingly, **M5** was A/C-ring-monohyroxylated demethylated AP.

M7

In PI mode, the MS^2 and MS^3 mass spectra of **M7** were not captured by the instrument in this study. In NI mode, its MS^2 mass spectrum showed fragment ions at *m/z* 286.0455, 257.0835, 242.0538, 191.0357 ($^{0,\ 4}B^- - 2H$ or $^{1,\ 4}B^- - 2H$) and 176.0137, which suggested that the newly added hydroxyl group might be located on A ring (carbon 1 or 2 or 4) or C ring (carbon 6 or 11a). Hence, **M7** was tentatively identified as 1/2/4/6/11a-monohyroxylated demethylated AP.

M9

In PI MS^2 mass spectrum of **M9**, the fragment ions at *m/z* 177.0555 ($^{1,\ 4}B^+ - 2H$), 153.0543 ($^{2,\ 3,\ 5}B^+ + H$ or $^{3,\ 4,\ 6}A^+ + H$), 139.0358 ($^{2,\ 4}A^+$ or $^{5,\ 6}B^+$), and 149.0635($^{1,\ 3,\ 7}B^+ - H$) implied that the newly added hydroxyl should be attached to A ring. **M9** was A-ring-monohyroxylated demethylated AP.

M12

The PI MS^2 and MS^3 mass spectra of **M12** were not captured by the instrument. In NI mode, its MS^2 mass spectrum showed fragment ions at *m/z* 286.0442, 271.0643, 268.0414, 256.0385,164.0157 ($^{2,\ 3,\ 7}A^- - 2H$), which suggested that the newly added hydroxyl group might be located on A ring or C ring. Thus, **M12** was A/C-ring-monohyroxylated demethylated AP.

M15

In PI MS^2 mass spectrum of **M15**, the fragment ions at *m/z* 177.0539 ($^{1,\ 4}B^+ - 2H$), 153.0533 ($^{2,\ 3,\ 5}B^+ + H$ or $^{3,\ 4,\ 6}A^+ + H$), 139.0372 ($^{2,\ 4}A^+$ or $^{5,\ 6}B^+$), and 163.0362 ($^{5,\ 6}A^+ - 2H$ or $^{2,\ 4}B^+ - 2H$) implied that the newly added hydroxyl should be attached to A ring or C ring. Therefore, **M15** was also A/C-ring-monohyroxylated demethylated AP.

M17

In PI MS^2 mass spectrum of **M17**, the fragment ions at *m/z* 153.0532 ($^{2,\ 3,\ 5}B^+ + H$ or $^{3,\ 4,\ 6}A^+ + H$), 285.0720, 177.0524 ($- H_2O^{1,\ 4}B^+$), 139.0354 ($^{2,\ 4}A^+$ or $^{5,\ 6}B^+$ or $^{1,\ 3,\ 7}A^+ + H$), 163.0379 ($^{5,\ 6}A^+ - 2H$ or $^{2,\ 4}B^+ - 2H$), 179.0308 ($^{6,\ 7}A^+ - 2H$), and 193.0482 ($- H_2O^{0,\ 4}B^+$ or $^{1,\ 4}B^+ - 2H$) implied that the newly added hydroxyl group should be attached to A ring or C ring. The PI MS^3 mass spectrum of positive ion at *m/z* 153.0532 showed fragment ions at *m/z* 138.0298, 125.0649, 93.0307, indicating that this ion was $^{2,\ 3,\ 5}B^+ + H$ and the newly added hydroxyl group should not be linked to carbon 6a on C ring or on B ring.

M20

The fragment ions at *m/z* 285.0638, 193.0449 ($- H_2O^{0,\ 4}B^+$ or $^{1,\ 4}B^+ - 2H$), 177.0541 ($- H_2O^{1,\ 4}B^+$), 163.0386 ($^{5,\ 6}A^+ - 2H$ or $^{2,\ 4}B^+ - 2H$), and 153.0535 ($^{2,\ 3,\ 5}B^+ + H$ or $^{3,\ 4,\ 6}A^+ + H$) in PI MS^2 mass spectrum of M20 indicated that the newly added hydroxyl group should be attached to A ring or C ring. The PI MS^3 mass spectrum of *m/z* 153.0535 showed fragment ions at *m/z* 138.0280 and *m/z* 125.0556, which indicated that *m/z* 153.0535 was $^{2,\ 3,\ 5}B^+ + H$ and the newly added hydroxyl group should not be linked to carbon 6a on C ring or on B ring.

Dihydroxylated metabolites-M6, M10, M11, M21

All of these four metabolites showed $[M + H]^+$ at *m/z* 333.09 in PI mode and $[M - H]^-$ at 331.08 in NI mode, which confirmed that their molecular weight were 332 Da. Calculated from the exact mass of $[M + H]^+$ and $[M - H]^-$, their molecular formulae were determined to be $C_{17}H_{16}O_7$. Thus, they should be dihydroxylated metabolites of AP.

M6

In PI MS^2 mass spectrum of **M6**, the fragment ions at *m/z* 179.0332 ($^{6,\ 7}A^+ - 2H$), 183.0658 ($^{2,\ 3,\ 5}B^+ + H$), 167.0688 ($^{2,\ 3,\ 7}B^+ + H$), 151.0386 ($^{3,\ 4,\ 6}A^+ - H$), and 181.0474 ($^{6,\ 7}A^+$ or $^{2,\ 3,\ 5}B^+ - H$) implied that one of the newly added hydroxyl groups should be attached to B ring and the other newly added hydroxyl group might be linked to A ring or C ring.

M10

The PI MS^2 and MS^3 mass spectra of **M10** were not captured by the instrument. In NI mode, the MS^2 mass spectrum of **M10** showed fragment ions at *m/z* 289.0722, 207.0672 ($C_{11}H_{11}O_4$, $^{1,\ 4}B^-$), 177.0196 ($C_9H_5O_4$, $^{6,\ 7}A^- - 2H$), and 192.0494. The product ion spectrum of negative ion at *m/z* 289.0722 showed fragment ions at 153.0590, 138.0305, 123.0097, and 230.0630. These fragment ions indicated that one newly added hydroxyl group should be attached to B ring and the other should be attached to A ring. Hence **M10** was A-ring-monohydroxylated and B-ring-monohydroxylated AP.

M11

The MS^2 and MS^3 mass spectra of **M11** in PI mode were not obtained by the instrument, because **M11** was very easy to loss an H_2O from its structure. This phenomenon implied that one of the newly added hydroxys might be linked to C ring. The MS^2 mass spectrum of $[M - H_2O + H]^+$ showed fragment ions at *m/z* 300.0060, 150.0247 ($- H_2O^{3,\ 4,\ 6}A^+$), indicating that the other newly added hydroxy should be linked to A ring. In NI mode, the MS^2 mass spectrum of **M11** showed fragment ions at *m/z* 316.0515, 313.0740, 289.0699, 271.0590, and 256.0270. The product ion spectrum of nega-

tive ion at *m/z* 289.0700 showed fragment ions at 274.0491, 259.0231 and 227.0340. These fragment ions indicated that the newly added hydroxyl group should not be linked to carbon 6a and carbon 11a on C ring. Thus, we tentatively identified **M11** as a dihydroxylated metabolite of astrapterocarpan (one hydroxy on A ring and the other linked to carbon 6.

M21

The MS^2 NI mass spectrum of **M21** showed the fragment ion at *m/z* 125.0239 ($^{1,4}A^- + 2H$, calculated to be $C_6H_5O_3$) as the only product ion, which indicated that one of the newly added hydroxys must be on A ring. In PI MS^2 mass spectrum of **M21**, the fragment ions at *m/z* 151.0383 ($^{3,4,6}A^+ - H$), 179.0324 ($^{6,7}A^+ - 2H$), 167.0701 ($^{2,3,7}B^+ + H$), and 181.0787 ($^{1,3,7}B^+ + H$) indicated that the other newly added hydroxy must be on B ring. Therefore, **M21** was also A-ring-monohydroxylated and B-ring-monohydroxylated AP.

Hydration metabolite-M14

M14 showed $[M + H]^+$ at *m/z* 319.1159 and $[M - H]^-$ at 317.1031, and its molecular formula was predicted to be $C_{17}H_{18}O_6$. Compared with the molecular formula ($C_{17}H_{16}O_5$) of the parent compound, we can identify **M14** as a hydration metabolite. Its structure should be 4, 7, 2′-trihydroxy-3′, 4′-dimethoxy-isoflavan. The MS^n data of **M14** were consistent with the identified structure.

Didemethylated metabolite-M16

M16 showed $[M + H]^+$ at *m/z* 273.0769 and $[M - H]^-$ at 271.0621, and its molecular formula was predicted to be $C_{15}H_{12}O_5$. Compared with the molecular formula ($C_{17}H_{16}O_5$) of the parent compound, we can identify **M16** as a didemethylated metabolite. Its structure should be 3, 9, 10-trihydroxy-pterocarpan. The MS^n data of **M16** were consistent with the identified structure.

Glucosylated metabolites-M18, M19

M18

The molecular formula of **M18** was determined to be $C_{23}H_{26}O_{11}$ based on its exact mass of $[M + H]^+$ at *m/z* 479.1530 and $[M - H]^-$ at 477.1394. In PI and NI MS^2 mass spectra, a neutral loss of 162.05 Da (elemental composition: $C_6H_{10}O_5$) indicated that **M18** was a glucosylated metabolite. Its aglycon had a molecular formula of $C_{17}H_{16}O_6$, which suggested that the aglycon was a monohydroxylated AP. In NI MS^3 mass spectrum of *m/z* 315.0836, two sequential losses of methyl radicals were observed, indicating that there were two methoxyl groups in the structure. The aglycon positive ion at *m/z* 317.1010 can fragment to the product ions of 191.0580 ($^{1,4}B^+ - 2H$) and 167.0684 ($^{2,3,5}B^+ + H$), indicating that the newly added hydroxyl group should be linked to A ring. Accordingly, **M18** was A-ring-monohydroxylated AP glucoside.

M19

In PI mode, **M19** showed $[M + H]^+$ at *m/z* 463.1597 and $[M + HCOOH - H]^-$ at 507.1496. Therefore, the molecular formula of **M19** was determined to be $C_{23}H_{26}O_{10}$ and the molecular formula of its aglycon was $C_{17}H_{16}O_5$. In NI MS^2 mass spectrum of *m/z* 507.1496, two sequential losses of methyl radicals were observed, indicating that there were two methoxyl groups in the structure of **M19**. Thus, **M19** was identified as AP-3-*O*-glucoside.

Monohydroxylated and dehydrogenated metabolite-M28

M28 showed $[M + H]^+$ at *m/z* 315.0861 and $[M - H]^-$ at 313.0727. Thus, its molecular formula was determined to be $C_{17}H_{14}O_6$. Its UV spectrum exhibited maximal absorption at 252 nm (14.68 mAU) and 340 nm (7.93 mAU), which was very different from those of pterocarpenes, coumestans and isoflavones, and was similar to that of benzofurans [24]. Accordingly, we suggested that the dehydrogenation reaction might occur at carbon 6 and carbon 6a, and a benzopyran structure was formed. After the careful analysis of its MS^2 and MS^3 mass spectra, and especially considering the characteristic fragment ions at *m/z* 137.0592 ($- 2CO^{6,7}B^+$) and 123.0411 ($- 2CO^{6,7}A^+$), we deduced that the newly added hydroxyl group should be attached to A ring.

Monohydroxylated, demethylated and dehydrogenated metabolites-M23, M29

M23

M23 showed $[M + H]^+$ at *m/z* 301.0698 and $[M - H]^-$ at 299.0558. Therefore, its molecular formula was predicted to be $C_{16}H_{12}O_6$. Its UV spectrum showed maximal absorption at 252 nm (13.47 mAU) and 340 nm (6.12 mAU), which was similar to that of benzofurans [24]. Accordingly, we suggested that a benzopyran structure was formed. Considering the characteristic fragment ions at *m/z* 123.0423 ($- 2CO^{6,7}A^+$ or $- 2CO^{6,7}B^+$), 163.0362 ($^{5,6}A^+$ or $^{2,4}B^+ - H$), we deduced that the newly added hydroxyl group should be attached to A ring.

M29

M29 showed $[M + H]^+$ at *m/z* 301.0718 and $[M - H]^-$ at 299.0550. Calculated from these exact masses, its molecular formula was determined to be $C_{16}H_{12}O_6$. Its UV spectrum showed maximal absorption at 247 nm (14.26 mAU), 334 nm (25.40 mAU) and a shoulder peak at 347 nm (19.80 mAU), which was very similar to that of pterocarpenes [24]. Accordingly, we suggested that the dehydrogenation reaction might occur at carbon 6a and carbon 11a, and a pterocarpene was formed. In PI MS^2 and MS^3 mass spectrum of **M29**, the quasi-molecular ion of $[M + H]^+$ can fragment to an ion at *m/z* 286.0449 and then this ion can fragment to ions at *m/z* 150.0247($^{2,4}B^+ + 2H$) and 137.0225($^{2,4}A^+ - 2H$). This indicated that the newly added hydroxyl group was on A ring.

Dimerized metabolites-M36, M39

The atom position numbering and the nomenclature for fragmentations of these dimers are shown in Fig. 3. Both **M36** and **M39** showed $[M + H]^+$ at *m/z* 599.19 in PI mode and $[M - H]^-$ at 597.17 in NI mode. Based on the exact masses of these quasi-molecular ions, their molecular formulae were determined to be $C_{34}H_{30}O_{10}$. Because the ions from intact monomer were not formed in their mass spectra, the linkage bond should not be O-O or C-O, and might be C-C. In PI mode, two sequential neutral losses of 178.06 Da ($C_{10}H_{10}O_3$, $^{2,4}B$) were observed from their MS^2 and MS^3 mass spectra.

Thus, the linkage between two monomers must be A ring↔A′ ring (A ring linked to A′ ring). Therefore, they were A-ring↔A′-ring-linked AP dimers.

Dimerized and monohydroxylated metabolites-M30, M32, M40

M30

Compared with the MS^n data of **M36** and **M39**, and considering the fragment ions at *m/z* 283.0611, 419.0992, 437.1205, and 461.1128 in MS^2 mass spectrum and the fragment ions at 255.0643, 283.0589, and 419.1032 in MS^3 mass spectrum of **M30**, we can deduce that the linkage between two monomers was A ring↔A′ring, and the newly added hydroxyl group was attached to A ring.

M32

The fragment ions at *m/z* 437.1251, 461.1161, 283.0565, and 179.0734 in MS^2 and MS^3 mass spectra of **M32** indicated that the linkage between two monomers was A ring↔A′ ring, and the newly added hydroxyl group was attached to A ring.

M40

In NI MS^2 mass spectrum of **M40**, a neutral loss of 206.0570 Da ($C_{11}H_{10}O_4$) from the quasi-molecular ion at *m/z* 613.1696 indicated that the linkage between two monomers was A ring↔A′ ring, and the newly added hydroxyl group was attached to A ring. In PI MS^2 mass spectrum of **M40**, the fragment ions at *m/z* 461.1337 and 437.1202 confirmed this conclusion.

Dimerized and didemethylated metabolites-M31, M33

M31

In NI MS^2 mass spectrum of **M31**, the fragment ion at *m/z* 325.0685($C_{18}H_{13}O_6$) indicated that the linkage between two monomers was A ring↔A′ ring, and one methyl from each monomer was lost.

M33

In PI MS^2 mass spectrum of **M33**, the fragment ions at *m/z* 461.1122, 449.1150, 437.1180, 419.1092, 313.0734, and 285.0638 indicated that the linkage between two monomers was A ring↔C′ ring, and one methyl from each monomer was lost.

Dimerized and demethylated metabolites-M34, M35, M37, M38, M41

All of these metabolites exhibited $[M + H]^+$ at *m/z* 585.17 in PI mode and $[M - H]^-$ at 583.16 in NI mode. According to the exact masses of their quasi-molecular ions, their molecular formulae were determined to be $C_{33}H_{28}O_{10}$. This suggested that they were dimerized and demethylated metabolites.

M34

The fragment ions at *m/z* 445.1265, 431.1193, 421.1275, and 407.1146($C_{23}H_{19}O_7$) in PI MS^2 mass spectrum of **M34**, and the fragment ions generated from 421.1275 at 299.0845, 269.0761, 255.0617, 243.0652, 239.0654, 215.0672, 191.0692, and 167.0687 in PI MS^3 mass spectrum of **M34** indicated that the linkage between two monomers was A ring↔A′ ring, and a methyl from one monomer was lost.

M35

The PI MS^2 mass spectrum of **M35** showed fragment ions at *m/z* 476.1524, 431.1128, 421.1179, 407.1122, and 343.1370, indicating that the linkage between two monomers was A ring↔C′ ring.

M37

The fragment ions at *m/z* 445.1265 ($C_{26}H_{21}O_7$), 407.1085 ($C_{23}H_{19}O_7$), 405.0936 ($C_{23}H_7O_7$), 299.0924 ($C_{17}H_{15}O_5$), and 241.0363 ($C_{14}H_9O_4$) in PI MS^2 mass spectrum of **M37** suggested that the linkage between two monomers was A ring↔A′ ring.

M38

The fragment ions at *m/z* 475.1289 ($C_{27}H_{23}O_8$), 463.1433 ($C_{26}H_{23}O_8$), 431.1121 ($C_{25}H_{19}O_7$), 407.1134 ($C_{23}H_{19}O_7$), 299.0924 ($C_{17}H_{15}O_5$), 285.0802 ($C_{16}H_{13}O_5$), and 191.0688 ($C_{11}H_{11}O_3$) in PI MS^2 mass spectrum of **M38** and the fragment ions at *m/z* 347.0757 ($C_{21}H_{15}O_5$) and 297.0820 ($C_{17}H_{13}O_5$) in PI MS^3 mass spectrum of **M38** (precursor ion at *m/z* 407.1134) suggested that the linkage between two monomers was A ring↔C′ ring.

M41

The fragment ions at *m/z* 463.1437 ($C_{26}H_{23}O_8$), 407.1134 ($C_{23}H_{19}O_7$), 391.1231, 299.0859 ($C_{17}H_{15}O_5$), 297.0820 ($C_{17}H_{13}O_5$), and 285.0738 ($C_{16}H_{13}O_5$) in PI MS^2 mass spectrum of **M41** and the fragment ions at 297.0740 ($C_{17}H_{13}O_5$) and 177.0534 ($C_{10}H_9O_3$) in PI MS^3 mass spectrum of **M41** (precursor ion at *m/z* 407.1134) suggested that the linkage between two monomers was A ring↔ C′ ring.

Discussion

In this paper, we reported the *in vitro* phase I metabolism of a pure pterocarpan (astrapteropan, AP) in rat hepatic S9 incubation system for the first time. Totally, 40 new metabolites and 1 new degradation product of AP were identified with the aid of NMR and HPLC-DAD-ESI-IT-TOF-MS^n techniques.

1. The reasons that we chose rat hepatic S9 incubation method to study the *in vitro* phase I metabolism of AP were: 1) hepatic S9 fraction was easier to prepare; 2) the metabolic activity of hepatic S9 was better than that of liver microsomes; 3) it was easier to scale up and could be used to isolate metabolites [18].

2. In our studies, we firstly isolated four compounds (**M1**–**M4**) from the rat hepatic S9 fraction incubated with AP. **M1** (6a-hydroxy-AP), **M2** [astrametabolin I, 1a-hydroxy-9, 10-dimethoxy-pterocarp-1(2), 4-diene-3-one], and **M3** (9-demethyl-AP, nissolin) are three new metabolites of AP, among which **M1** and **M2** are new compounds. **M4** (4-methoxy-astraisoflavan) is a new degradation product of AP.

M2 had a rearranged A ring and had a hydroxy at carbon 1a on A ring. It has been reported that monohydroxylation of carbon 1a and rearrangement of A ring could happen when medicarpin (a pterocarpan) was incubated with mycelium preparations or with crude protein extracts of the fungus [25-27]. Our results indicate that this kind of metabolic reaction can also happen in hepatic S9 fraction and the fungus could be used to prepare such kind of metabolites. As far as we know,

this is the first report on this kind of biotransformation of pterocarpans occurs in animals or their tissues.

M4 could not be detected in the sample of test group by HPLC-DAD-ESI-IT-TOF-MS^n analysis, which indicated that it might be a degradation product of AP during isolation process. According to literature [28], the formation mechanism of **M4** might be photolysis and solvolysis by methanol. To confirm this deduction, we dissolved AP in methanol and then eluted it on Sephadex LH-20 column with methanol, and found that **M4** was formed under this condition.

3. We tentatively identified 40 new metabolites of AP formed in rat hepatic S9 incubation medium by HPLC-DAD-ESI-IT-TOF-MS^n analysis.

The representative BPCs of the samples in NI mode are shown in Fig. 2, and the metabolic pathways of AP are proposed and shown in Fig. 5. From Fig. 2C, we could find that the most of AP was transformed to astraisoflavan (identified by direct comparison with astraisoflavan standard isolated from *Astragali* Radix by the authors) in the medium without rat hepatic S9 fraction, and no other products could be detected. While incubated with rat hepatic S9 fraction, this transformation could not be observed. This indicates that AP preferentially undergo metabolism by rat hepatic S9, rather than undergo degradation to astraisoflavan.

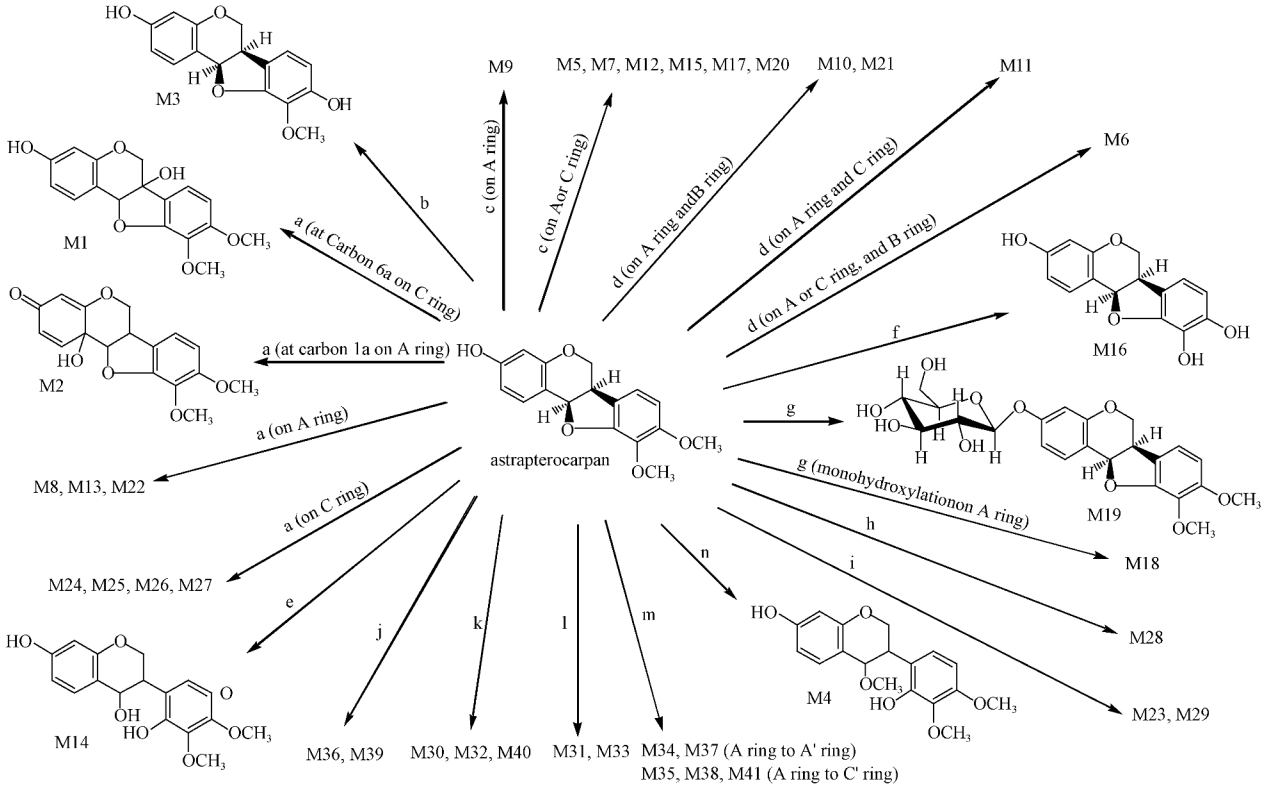

a: monohydroxylation; b: demethylation; c: demethylation and monohydroxylation; d: dihydroxylation; e: hydration; f: didemethylation; g: glucosylation; h: monohydroxylation on A ring and dehydrogenation at carbon 6 and 6a; i: monohydroxylation on A ring and demethylation and dehydrogenation; j: dimerization (A ring linked to A' ring); k: dimerization (A ring linked to A' ring) and monohydroxylation on A ring; l: dimerization and didemethylation (from B ring and B' ring); m: dimerization and demethylation; n: degradation (photolysis and solvolysis by methanol)

Fig. 5 The proposed metabolic pathways of astrapterocarpan in rat hepatic S9

Among these 40 metabolites, 23 metabolites were monohydroxylated products, and 12 of them (**M2**, **M8**, **M9**, **M13**, **M18**, **M22**, **M23**, **M28**, **M29**, **M30**, **M32**, **M40**) were hydroxylated on A ring, 6 of them (**M5**, **M7**, **M12**, **M15**, **M17**, **M20**) were hydroxylated on A ring or C ring, and the last 5 of them (**M1**, **M24**, **M25**, **M26**, **M27**) were hydroxylated on C ring. But the hydroxylation occurred on the B ring was not found. This indicates that the monohydroxylation has the structure selectivity order as follows: A ring, C ring, and B ring.

Four metabolites were dihydroxylated products, and 3 of them (**M6**, **M10**, **M21**) were hydroxylated on B ring and A or C ring, which suggest that B ring also can be hydroxylated when the second hydroxy is introduced into the structure.

Fifteen metabolites (**M3**, **M5**, **M7**, **M9**, **M12**, **M15**, **M17**, **M20**, **M23**, **M29**, **M34**, **M35**, **M37**, **M38**, **M41**) were monodemethylated products, and 3 metabolites (**M16**, **M31**, **M33**) were didemethylated products, which indicate that demethylation is also a principal metabolic reaction for AP, and monodemethylation is the main reaction.

Totally 12 dimerized metabolites were found, and the linkage bond between two monomers in their structures was C–C. Eight of them (**M30**, **M31**, **M32**, **M34**, **M36**, **M37,** **M39**, **M40**) had the linkage form of A ring↔A′ ring, the other four (**M33**, **M35**, **M38**, **M41**) had the linkage form of A ring↔C′ ring. All the monomers in their structures keep the

skeleton of pterocarpans. Many dimers of flavonoids have been isolated from plants, but only one bipterocarpan has been isolated from natural source (*Millettia pachyloba*, a plant), and the monomers are linked via an oxygen atom [29]. Therefore, it is for the first time that we found the dimerization of pterocarpans can occur in animal metabolic experiment. Furthermore, this indicates that rat hepatic S9 may be used to biosynthesize bipterocarpans.

Two glucosylated metabolites were identified in this research, indicating that rat hepatic S9 has the ability to glucosylate pterocarpans.

4. The relative content of each metabolite could be determined by the percentage of its peak area to the total peak area of 40 metabolites determined from BPC in NI mode. From the value shown in Table 2, we can find that the major metabolites of AP are **M25** (6-hydroxy-AP, 19.62%), **M26** (diastereomer of **M25**, 14.10%), **M2** (astrametabolin I, 14.01%), **M3** (9-demethyl-AP, 11.49%), **M17** (1/2/4/6/11a-monohydroxylated demethylated AP, 8.35%), and **M39** (AP dimer, 4.96%). Hence, it can be considered that the major metabolic pathways of AP in rat hepatic S9 fraction are monohydroxylation, monodemethylation and dimerization.

5. It has been reported that the metabolites of isoflavones owned similar bioactivities to those of their prototypes [30-31]. Whether these metabolites have the similar pharmacological activities to those of AP needs further research.

6. Although we could not elucidate the exact structures of all metabolites just by current LC-MS technique, the structures of **M1**, **M2**, **M3**, **M4**, **M14**, **M16**, **M19** still could be elucidated unequivocally because of the aid of NMR technique or the solely metabolic site. By searching all possible structures of each metabolite in SciFinder database, we found that: among 40 new metabolites of AP, **M3** and **M19** were known compounds, and **M23**, **M29** might be new compounds or known compounds; the other 36 metabolites were new compounds.

Conclusion

In summary, the *in vitro* metabolism of a pure pterocarpan (AP) was studied for the first time by rat hepatic S9 incubation. The metabolite profile of AP was obtained, and 40 new metabolites were identified by NMR and HPLC-DAD-ESI-IT-TOF-MS^n techniques. The metabolic reactions of AP in rat hepatic S9 fraction were found to be hydroxylation, demethylation, dimerization, glucosylation, dehydrogenation, and hydration, among which the first three were major metabolic reactions. Among 40 new metabolites of AP, 36 metabolites were new compounds. The new degradation product (**M4**, 4-methoxy-astraisoflavan) was also a new compound. Whether these metabolic pathways of AP also exist *in vivo* was unclear and required for further study. Our findings would provide a solid basis for further studies on the metabolism of other pterocarpans in animals.

References

[1] Liu PP, Shan GS, Zhang F, *et al*. Metabolomics analysis and rapid identification of changes in chemical ingredients in crude and processed Astragali Radix by UPLC-QTOF-MS combined with novel informatics UNIFI platform [J]. *Chin J Nat Med*, 2018, **16**(9): 714-720.

[2] Li AP, Li ZY, Qu TL, *et al*. Nuclear magnetic resonance based metabolomic differentiation of different Astragali Radix [J]. *Chin J Nat Med*, 2017, **15**(5): 363-374.

[3] Robeson DJ, Ingham JL. New pterocarpan phytoalexins from *Lathyrus nissolia* [J]. *Phytochemistry*, 1979, **18**(10): 1715-1717.

[4] Goda Y, Katayama M, Ichikawa K, *et al*. Inhibitors of prostaglandin biosynthesis from *Dalbergia odorifera* [J]. *Chem Pharm Bull (Tokyo)*, 1985, **33**(12): 5606-5609.

[5] Spencer GF, Jones BE, Plattner RD, *et al*. A pterocarpan and two isoflavans from alfalfa [J]. *Phytochemistry*, 1991, **30**(12): 4147-4149.

[6] Li G, Wang J, Li X, *et al*. Isolation and identification of pterocarpans and isoflavones from the pericarp of *Sphaerophysa salsula* DC. [J]. *Chin J Med Chem*, 2003, **13**(4): 215-218.

[7] Li C, Liu J, Di D, *et al*. Analysis of three flavonoids in *Oxytropis kansuensis* Bunge by RP-LC-DAD coupled with weighted least-squares linear regression [J]. *Chromatographia*, 2008, **68**(9/10): 773-779.

[8] Niu D, Li Y, Wu X, *et al*. Pterocarpan derivatives from *Clinopodium urticifolium* and their cytotoxicity [J]. *Asian J Chem*, 2013, **25**(17): 9672-9674.

[9] Sung CK. Inhibitors of sterol biosynthesis from *Astragalus membranaceus* Bunge [C]. *Recent Advances in Natural Products Research, Proceedings of the International Symposium on Recent Advances in Natural Products Research, 3rd*, Seoul, Republic of Korea, 1999, 69-73.

[10] Okawara S, Nagao T, Yamagishi T, *et al*. Pterocarban for promoting bone formation and as antiarteriosclerotic and health food. JP, 2003155236 [P]. 2003.

[11] Ohkawara S, Okuma Y, Uehara T, *et al*. Astrapterocarpan isolated from *Astragalus membranaceus* inhibits proliferation of vascular smooth muscle cells [J]. *Eur J Pharmacol*, 2005, **525**(1-3): 41-47.

[12] Zhang W, Xu F, Wang D, *et al*. Buyang Huanwu Decoction ameliorates ischemic stroke by modulating multiple targets with multiple components: *in vitro* evidences [J]. *Chin J Nat Med*, 2018, **16**(3): 194-202.

[13] Yang D, Cai S, Liu H, *et al*. On-line identification of the constituents of Buyang Huanwu decoction in pig serum using combined HPLC-DAD-MS techniques [J]. *J Chromatogr B Analyt Technol Biomed Life Sci*, 2006, **831**(1-2): 288-302.

[14] Xu F, Zhang Y, Xiao S, *et al*. Absorption and metabolism of Astragali Radix decoction: in silico, *in vitro*, and a case study *in vivo* [J]. *Drug Metab Dispos*, 2006, **34**(6): 913-924.

[15] Li C, Qi L, Li P, *et al*. Identification of metabolites of Danggui Buxue Tang in rat urine by liquid chromatography coupled with electrospray ionization time-of-flight mass spectrometry [J]. *Rapid Commun Mass Spectrom*, 2009, **23**(13): 1977-1988.

[16] Li C, Qi L, Li P. Correlative analysis of metabolite profiling of Danggui Buxue Tang in rat biological fluids by rapid resolution LC-TOF/MS [J]. *J Pharm Biomed Anal*, 2011, **55**(1): 146-160.

[17] Zhang Y, Xu F, Liang J, *et al*. Isoflavonoids from roots of *Astragalus membranaceus* var. *mongholicus* [J]. *Chin J Chin Mater Med*, 2012, **37**(21): 3243-3248.

[18] Wu W, McKown LA. *In vitro drug metabolite profiling using*

hepatic S9 and human liver microsomes [M]. Humana Press Inc, Totowa, 2004: 163-184.

[19] Zhao C, Shao QJ, Ma ZQ, *et al*. Physical and chemical characterizations of corn stalk resulting from hydrogen peroxide presoaking prior to ammonia fiber expansion pretreatment [J]. *Ind Crop Prod*, 2016, **83**: 86-93.

[20] Yi T, Zhu L, Tang YN, *et al*. An integrated strategy based on UPLC-DAD-QTOF-MS for metabolism and pharmacokinetic studies of herbal medicines: Tibetan "Snow Lotus" herb (*Saussurea laniceps*), a case study [J]. *J Ethnopharmacol*, 2014, **153**(3): 701-713.

[21] Denny TP, VanEtten HD. Metabolism of the phytoalexins medicarpin and maackiain by *Fusarium solani* [J]. *Phytochemistry*, 1982, **21**(5): 1023-1028.

[22] Lee EJ, Yean MH, Jung HS, *et al*. Phytochemical studies on Astragalus root (2)-flavonoids and a lignin [J]. *Nat Prod Sci*, 2008, **14**(2): 131-137.

[23] Simons R, Vincken JP, Bohin MC, *et al*. Identification of prenylated pterocarpans and other isoflavonoids in *Rhizopus spp*. elicited soya bean seedlings by electrospray ionisation mass spectrometry [J]. *Rapid Commun Mass Spectrom*, 2011, **25**(1): 55-65.

[24] Yang M, Wang W, Sun J, *et al*. Characterization of phenolic compounds in the crude extract of *Hedysarum multijugum* by high-performance liquid chromatography with electrospray ionization tandem mass spectrometry [J]. *Rapid Commun Mass Spectrom*, 2007, **21**(23): 3833-3841.

[25] Denny TP, VanEtten HD. Tolerance by *Nectria haematococca* MP VI of the chickpea (*Cicer arietinum*) phytoalexins medicarpin and maackiain [J]. *Physiol Plant Pathol*, 1981, **19**(3): 419-437.

[26] Kraft B, Schwenen L, Stoeckl D, *et al*. Degradation of the pterocarpan phytoalexin medicarpin by *Ascochyta rabiei* [J]. *Arch Microbiol*, 1987, **147**(2): 201-206.

[27] Tenhaken R, Salmen HC, Barz W. Purification and characterization of pterocarpan hydroxylase, a flavoprotein monooxygenase from the fungus *Ascochyta rabiei* involved in pterocarpan phytoalexin metabolism [J]. *Arch Microbiol*, 1991, **155**(4): 353-359.

[28] Van der Merwe PJ, Rall GJH, Roux DG. Novel isoflavan-pterocarpan interconversions: some structural requirements for cyclization [J]. *J Chem Soc Chem Commun*, 1978, (6): 224-225.

[29] Mai HD, Nguyen TT, Pham VC, *et al*. Cytotoxic prenylated isoflavone and bipterocarpan from *Millettia pachyloba* [J]. *Planta Med*, 2010, **76**(15): 1739-1742.

[30] Nestel P, Fujii A, Zhang L. An isoflavone metabolite reduces arterial stiffness and blood pressure in overweight men and postmenopausal women [J]. *Atherosclerosis*, 2007, **192**(1): 184-189.

[31] Liang X, Wang X, Li Z, *et al*. Improved *in vitro* assays of superoxide anion and 1, 1-diphenyl- 2-picrylhydrazyl (DPPH) radical-scavenging activity of isoflavones and isoflavone metabolites [J]. *J Agric Food Chem*, 2010, **58**(22): 11548-11552.

Cite this article as: ZHANG Ya-Zhou, XU Feng, DONG Jing, LIANG Jing, HASHI Yuki, LIU Guang-Xue, LI Yao-Li, SHANG Ming-Ying, WANG Xuan, CAI Shao-Qing. Profiling the metabolites of astrapterocarpan in rat hepatic 9000g supernatant [J]. *Chin J Nat Med*, 2019, **17**(11): 842-857.